# Experimental Comparison of Methods for Differential Geometric Properties Evaluation in Triangular Meshes

Luca Di Angelo[1] and Paolo Di Stefano[2]

[1]L'Aquila University, luca.diangelo@univaq.it
[2] L'Aquila University, paolo.distefano@univaq.it

**ABSTRACT**

This paper deals with the investigation of the stability and the accuracy of the most important methods to estimate the parameters that are involved in the shape recognition process of tessellated surfaces. For this purpose, four approaches to estimate the differential geometric properties of tessellated surfaces are systematically examined (namely, *simple* and *extended quadric fitting methods*, *Rusinkiewicz's* method and *Meyer discrete* method). A set of test cases has been designed in order to investigate the sensitivity of those methods to factors such as noise in point location, surface typology (chosen between those types that usually define the boundary of mechanical parts such as: planes, cylinders, spheres, cones and tori), mesh resolution and mesh regularity. Based on the results obtained, some criticism of the analyzed methods is made and some guidelines are provided in order to choose the most robust and reliable method in relation to the surface typology, quality of the mesh and noise in point location.

**Keywords:** triangular meshes, curvature estimation, shape recognition.
**DOI:** 10.3722/cadaps.2011.193-210

## 1 NOMENCLATURE

**p** : Point of the tessellated surface;
**n**(**p**) : Unit vector normal to the tessellated surface at a vertex **p**;
$k_1$, $k_2$ : Principal curvatures with $k_1 > k_2$;
**FS**(**p**): $\mathbf{FS}_{k1} = \mathbf{p} - \frac{\mathbf{n}}{k_1}$ $\mathbf{FS}_{k2} = \mathbf{p} - \frac{\mathbf{n}}{k_2}$ focal points related to principal curvature $k_1$ and $k_2$
*H*: Mean curvature;
*K*: Gaussian curvature;
*R*: Curvedness measure = $\sqrt{k_1^2 + k_2^2}$ .

## 2 INTRODUCTION

Shape recognition in geometric models defined by triangular meshes is a very complex task to accomplish. It is commonly required for geometric feature recognition in reverse engineering, geometric data smoothing and tolerances verification. A tessellated geometric model is a collection of adjacent planar triangular facets which define a closed (and) oriented Eulerian surface [23]. Shape recognition is a way of simplifying a geometric model described by triangular facets, by reducing it to a collection of a few adjacent smooth surfaces, each characterized by a specific geometric type. For this purpose, it is required that a set of adjacent planar triangular facets be recognized as pertaining to a unique smooth surface. In other words, a polyhedral surface is likened to a smooth surface whose points have specific characteristics: they are of the same type (elliptic, flat, hyperbolic, parabolic and umbilical) and have a specific value for some geometric parameters (principal curvatures, focal points' location and principal directions). A smooth surface involves the concept of regular point: each point in a smooth surface is regular and vice versa, any point of a surface is said to be regular if its neighborhood can be represented by a smooth function. This property of the points of a surface can be projected to the vertex of a tessellated surface by performing a recognition process of the smoothness property of the region around the vertex. Shape recognition is typically carried out by locally analyzing some differential properties of the surface under examination. These properties have to be deduced from discrete data retained in the mesh's vertices' location under the hypothesis that they are regular points. Regular point recognition is therefore necessary and it is a preliminary stage in any shape recognition approach in tessellated models. A review of methods for regular point recognition is presented in [28].

Principal curvatures are the most important differential properties required to identify the point type and, therefore, shape geometry; other local surface properties, such as normal vector and focal points at vertex, can be necessary to identify a more specific type of surface geometry. The estimation of differential properties at the vertices of a triangular mesh is affected by uncertainties and errors. These uncertainties depend mainly on some factors which characterize the tessellated surface such as: mesh resolution, non-uniformity of the triangles' dimensions and the number of triangles sharing each vertex (valence). These factors affect the recognition process depending on the typology of the surface to be recognized (plane, cylinder, cone, sphere, tori). Uncertainty in shape recognition can also be due to an error in point location. Point location is affected by measurement errors and by the manufacturing errors of the acquired model. A further source of error can be the merging process of point clouds that are acquired in different positions of the object. Noise deriving from the errors in point location can be partially compensated by a pre-smoothing of the mesh, but, on the other hand, it can significantly modify the local properties of the tessellated surface.

The literature on curvature estimation methods for triangular meshes is wide and voluminous. In the next section, a survey of these methods is presented. Magid et al [17] provide a comparison of four different methods for Gaussian and mean curvature estimation on triangular meshes. However, there is a shortcoming in such a comparison inasmuch as they do not systematically analyze all the significant mesh parameters which may affect the performance of the methods for curvature estimation. Gatzke and Grimm [7], in order to estimate the accuracy and stability of the most important methods for Gaussian curvature estimation, evaluate the effects of some mesh parameters (resolution, valence, regularity and noise). While it is true that Gaussian curvature is an important parameter, it is not the only one involved in shape recognition.

The present work will demonstrate that the diverse methods show different performances in the evaluation of the typical parameters involved in shape recognition; the analyses of the performances in Gaussian curvature estimation do not completely characterize these methods. The investigation, concerning curvature estimation methods, is focused on shape recognition, so some particular differential properties have been considered (normal to surface, focal points, Mean and Gaussian curvatures). Furthermore, the study is oriented to a practical application where the tessellated model can also be affected by noise in point location (it is typical of scanned objects). For this purpose, sensitivity to the noise factors of some parameters specifically suited for shape recognition is examined.

## 3 CURVATURE ESTIMATION METHODS

In the last few years several methods have been developed to directly estimate curvature at the vertex of triangular meshes [1], [16], [24], [26], [29], [31]. These methods can be classified into two main groups: *fitting* and *discrete* methods. *Fitting methods*, on the one hand, involve finding an analytic function that fits the mesh locally and whose curvature is well-defined. *Discrete* methods, on the other hand, develop either a direct approximation for the curvature, or an approximation of the curvature tensor, from which curvature and curvature directions can be calculated. These approaches require that a certain neighborhood of each vertex **p** of the mesh be considered. In particular, the *discrete* methods use, commonly, *1-ring neighborhoods*, whereas *fitting methods* can involve neighborhoods of higher order. In the latter case, the selection of the order of neighborhood rings significantly affects results: neighborhoods of lower order provide a better estimation of differential properties for synthetic meshes, whereas, as the order of neighborhood rings increases, the estimation is rougher although less sensitive to noise. The *1-ring neighborhood* of **p** is constituted by all triangles having **p** as vertex; $N_1(\mathbf{p})$ is the set of vertices belonging to *1-ring neighborhood* of **p**. The *valence* $n_v$ is the number of vertices in $N_1(\mathbf{p})$. A higher order of neighborhood of **p** is denoted with $N_j(\mathbf{p})$ where $j$ is the order.

### 3.1 Discrete Methods

*Discrete* methods work directly on the tessellated surface without a local fitting and the analytical evaluation of its local properties. The local geometric properties at the vertices of the triangulated surface are derived as spatial averages of the corresponding properties on a well-defined region around vertices.

A large number of papers deal with approaches based on the estimation of tensor of curvature such as Taubin's work [30]. He firstly demonstrated that the following symmetric 3x3 matrix:

$$\mathbf{M_p} = \frac{1}{2\pi}\int_{-\pi}^{\pi} k(\mathbf{T}_\theta)\cdot \mathbf{T}_\theta \cdot \mathbf{T}_\theta{}^t \cdot d\theta \tag{1}$$

has two eigenvectors that are the principal directions of the surface in **p**. The eigenvalues of $M_p$ can be related to principal curvatures. In (1), $\mathbf{T}_\theta$ is the unit-length tangent vector to the surface $S$ at point **p**, rotated by the angle $\theta$ with respect to the first principal direction and $k(\mathbf{T}_\theta)$ is the normal curvature of $S$ at **p** in the direction $\mathbf{T}_\theta$.

For a tessellated surface, Taubin [30] proposed the following approximation of the equation (1):

$$\mathbf{M_p} = \sum_{\mathbf{p}_j \in N_1(\mathbf{p})} w_j k_j \mathbf{T}_j \mathbf{T}_j{}^t \tag{2}$$

where $w_j$ are weight factors which are proportional to the normalized sum of the area of all triangles incident to both vertices **p** and $\mathbf{p}_j$; $k_j$ is the normal curvature in the direction of $\boldsymbol{T}_j$, that is, the unit-length tangent vector obtained by projecting the vector ($\mathbf{p}$-$\mathbf{p}_j$) onto the tangent plane of the surface in **p**. The expression of $k_j$ is approximated as follows:

$$k_j = \frac{2\cdot \mathbf{n}\cdot(\mathbf{p}-\mathbf{p}_j)}{\left\|\mathbf{p}-\mathbf{p}_j\right\|} \tag{3}$$

In literature, modifications of the Taubin's methods are proposed by Hameiri and Shimshoni [11] and Page et al [24]. Rusinkiewicz [27] verified that these methods are accurate only when the directions of the edges incident to **p** are uniformly spaced. A variant of the tensor averaging method is proposed by Cohen-Steiner et al. [5]; the original contribution of this study is that the curvature tensor is obtained by using the theory of *normal cycles*. Rusinkiewicz [27], proved that the tensor averaging method proposed by Cohen-Steiner et al. [5] yields inaccurate results even for densely-spaced synthetic meshes.

A second set of *discrete* methods evaluates the Gaussian and Mean curvatures at vertex **p**, by extending the definitions of differential quantities in the continuous case to discrete meshes performing a spatial average. This average is consistent when the mesh is constituted by non-degenerate triangles (triangles with non-null area). According to this approach, Gaussian curvature is estimated by the following formula, which is a consequence of the *Gauss-Bonnet* theorem [6]:

$$\iint_A K dA = \left( 2\pi - \sum_{i=1}^{\#f} \vartheta_i \right) \tag{4}$$

The left-hand term in (4) is the integral of the Gaussian curvature over an integration area $A$ around **p**, which is bounded by a closed curve on $S$ which consists of a set of geodesic arcs. In (4) $\#f$ is the number of triangles belonging to *1-ring neighborhood* of **p** and $\vartheta_i$ is the angle at **p** of the *i-th* triangle. The right-hand term in (4) is referred to as *angular defect* at **p**. This name is due to its geometrical meaning: it is the complement of a round angle of the sum of the angles in **p** of the triangles belonging to the *1-ring neighborhood*. Under the hypothesis that Gaussian curvature is constant on an area $A$ around **p**, $K$ can be estimated as follows:

$$K = \frac{\left( 2\pi - \sum_{i=1}^{\#f} \vartheta_i \right)}{\sum_{i=1}^{\#f} A_i} \tag{5}$$

$A_i$ is the area of a properly selected portion of the *i-th* triangle in the *1-ring neighborhood* of **p**. In order to estimate $A_i$ two main criteria have been presented in literature. Lin and Perry [15] proposed estimating $A_i$ as the portion of the triangle area bounded by connecting the edge midpoints to the barycenter ($A_i$ is one-third of the whole triangle area). Borrelli el al. [2] evinced that when the mesh triangles are *flattened geodesic triangles* this criterion is correct if contribution terms of order higher than two in the triangles' dimensions can be neglected. In a *flattened geodesic triangle* [2] the edges have the same length as the related arcs of a geodesic triangle on the original smooth surface. Meyer et al. [21] assumed that $A_i$ was equal to the *Voronoi cell* area of the triangle (see figure 1.a) and showed that "*this region provides provably tight error bounds for the discrete operators by comparing the local spatial average of Gaussian curvature with the actual pointwise value*". However, Meyer et al. did not make any assumption about an important prerequisite when using (5), whose validity is confirmed only when the integration area is bounded by geodesic curves. Xu [34] verified, by analyzing some synthetic meshes, that the Gaussian curvature estimation based on the *Voronoi cell* area is, in general, better than one based on barycentric area.

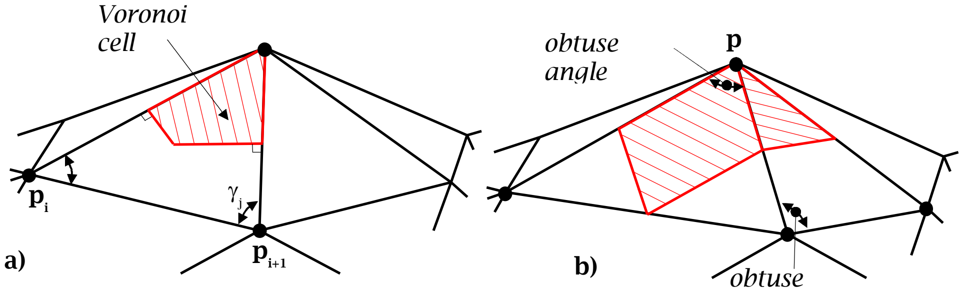


Fig. 1: The *Voronoi cell* (a) and the integration cells (b) associated, respectively, to a non-obtuse triangle and to the two different typologies of obtuse triangles of the *1-ring neighborhood* of p.

Meyer et al. [21], also, proposed a discrete method to estimate Mean curvature. They use the *Mean Curvature Normal* operator (**H**) at the vertex **p**, also known as *Laplace-Beltrami* operator:

$$\mathbf{H}(\mathbf{p}) = 2 \cdot H \cdot \mathbf{n} \tag{6}$$

On a triangular mesh, the integral of the *Mean Curvature Normal* operator over the area $A$ can be expressed as a function of the nodes' coordinates and the internal angles of triangles ($\alpha_j$ and $\beta_j$ as in Figure 2):

$$\iint_A \mathbf{H}(\mathbf{p}) dA = \frac{1}{2} \sum_{j \in N_1(\mathbf{p})} \left( \cot\alpha_j + \cot\beta_j \right) \cdot \left( \mathbf{p} - \mathbf{p}_j \right) \tag{7}$$

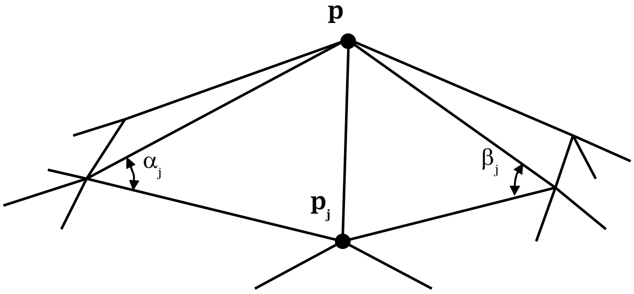


Fig. 2: The angles opposite an edge belonging to *1-ring neighborhood* of **p**.

Under the hypothesis that *Mean Curvature Normal* operator is constant on an area $A$ around **p**, **H** can be estimated as follows:

$$\mathbf{H}(\mathbf{p}) = \frac{\frac{1}{2}\sum_{j\in N_1(\mathbf{p})}\left(\cot\alpha_j + \cot\beta_j\right)\cdot\left(\mathbf{p}-\mathbf{p}_j\right)}{\sum_{i=1}^{\#f} A_i} \tag{8}$$

The effectiveness of the method proposed by Meyer et al. can be seen in some evidences as discussed in [21], where the authors justify choosing to use the *Voronoi cell* by estimating the error in $H$ and $K$ and verifying that this error is minimized in the case of the area of the Voronoi cell. The authors notice that this approach gives rise to some problems when triangles are obtuse. For these cases they proposed the following two empirical criteria to evaluate the area $A_i$:

- if the angle is obtuse at vertex **p**, the cell boundaries connect the midpoint of each edge incident to **p** to the midpoint of the edge opposite to the obtuse angle (see Figure 1 b);
- if the obtuse angle is not placed at vertex **p**, the cell boundary connects the midpoints of the two edges incident to **p** (see Figure 1 b).

The resulting area of each vertex **p**, denoted as $A_{mixed}$, is obtained by summing the contributions of the area of the integration cells associated to triangles belonging to *1-ring neighborhood* of **p**.

### 3.2 Fitting methods

*Fitting methods* estimate curvature by effecting a local approximation of the vertices of the triangular mesh with a smooth curve or surface and then deriving the second-order differential quantities from that. This surface reproduces locally the properties of the hypothetical original smooth surface from which the tessellated model has originated; curvatures of the fitting primitive are computed and assumed as curvatures of the triangular mesh.

One of the early *fitting methods* for curvature estimation was proposed by Chen and Schmitt in [4]; this approach is based on the Euler's formula, which links the curvature on the normal section of a surface to its principal curvatures:

$$k(\mathbf{T}_\theta) = k_1\cdot\cos^2(\vartheta) + k_2\cdot\sin^2(\vartheta) \tag{9}$$

where $\boldsymbol{T}_\theta$ is the tangent to the surface at point **p** in the direction individuated by the angle $\theta$ with respect to the first principal direction (related to $k_1$). Given a point **p** and its neighboring points, it is possible to identify pairs of opposite points to **p**. In order to limit the effects of the computation error for angle $\theta$, Chen and Schmitt in [4] proposed choosing point pairs that are as close as possible to the normal sections of the surface passing through **p**. For each pair identified, the circle passing through the two points given and **p** is calculated and its curvature is assumed as a curvature of the normal section of the surface in **p**. By using at least three such pairs, a system of Euler's equations can be constructed; the solution of this system are the curvatures $k_1$ and $k_2$. Similar algorithms, based on circle fitting, were introduced by Martin [18] and Krsek et al. [14]. Hameiri et al. [11] demonstrated several limitations emerging from this approach: first, insufficient accuracy whenever the normal section passing through the analyzed node differs from a circle and, second, the assumption that the section containing **p** and the chosen opposite points is a normal section of the surface in **p**.

The polynomials of second degree (paraboloid) are the most used fitting surfaces for curvature evaluation [8], [16], [22], [25], [26], [29], [33]; Krsek et al. [14] verified that polynomials of higher degree do not introduce significant advantages. By using the paroboloid fitting, the triangular mesh is locally approximated by a quadric surface patch whose analytical form is as follows:

$$\zeta = a\xi^2 + b\xi\psi + c\psi^2 + d\xi + e\psi + f \tag{10}$$

in the local coordinate system ($\xi$, $\psi$, $\zeta$) with origin at vertex **p** and $\zeta$-axis that overlaps the unit vector normal **n** evaluated at vertex **p** (see Figure 3). This approach requires a preventive estimation of the normal at the vertex. The correct identification of the normal to the surface in **p** plays an important role in the results of this curvature estimation method. In section 3, some methods of surface normal estimation are compared.

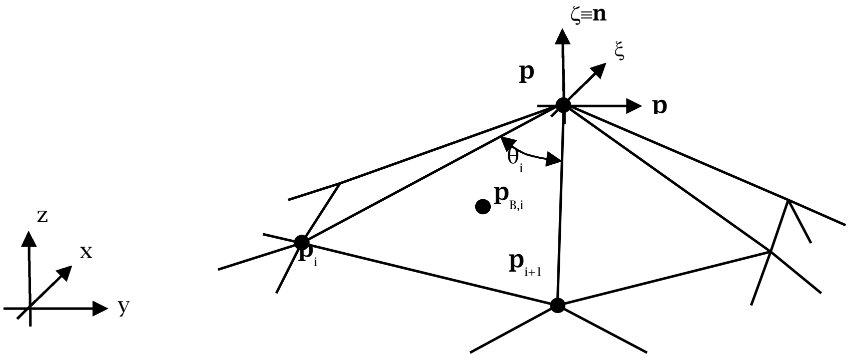


Fig. 3: Piecewise-linear surface and the local coordinate system (ξ, ψ, ζ).

The coefficients of the quadric in (10) are determined by solving the following redundant equation system with a least-squares approach:

$$\begin{bmatrix} \xi_1^2 & \xi_1\psi_1 & \psi_1^2 & \xi_1 & \psi_1 & 1 \\ \vdots & \vdots & \vdots & \vdots & \vdots & \vdots \\ \vdots & \vdots & \vdots & \vdots & \vdots & \vdots \\ \vdots & \vdots & \vdots & \vdots & \vdots & \vdots \\ \vdots & \vdots & \vdots & \vdots & \vdots & \vdots \\ \xi_n^2 & \xi_n\psi_n & \psi_n^2 & \xi_n & \psi_n & 1 \end{bmatrix} \cdot \begin{bmatrix} a \\ b \\ c \\ d \\ e \\ f \end{bmatrix} = \begin{bmatrix} \zeta_1 \\ \vdots \\ \vdots \\ \vdots \\ \vdots \\ \zeta_n \end{bmatrix} \tag{11}$$

It is important to notice that, in order to resolve this equation system, the valence **p** should not be lower than 6. For this reason, in some cases *1-ring neighborhood* is not sufficient and a higher order of neighborhood must be identified.

Equation (10) represents the complete form of the fitting paraboloid (also called *full quadric*). Different quadric functions can be obtained by deleting selected coefficients in (10) [25], [29]. Setting the $f$ term as zero means imposing the passage of the paraboloid through the vertex **p** (*extended quadric*). If $d$ and $e$ coefficients are also zero, the axis of the fitting paraboloid coincides with the $\zeta$-axis (*simple quadric*). Different quadric forms effect different approximations and, consequently, have different results in terms of differential quantities.

More recently, Razdan and Bae [26] suggested using a biquadratic Bèzier surface. Contrary to the paraboloid, the *Bèzier patch* involves several advantages such as higher flexibility (the parametric approach makes it possible to easily increase the fitting function degree) and the possibility to smooth noisy data. However, it requires the valence of the vertex under examination to be at least 9, so the $N_1$(**p**) is not sufficient.

Thiesel et al. in [31] proposed a *fitting method* based approach called *Normal based estimation of the curvature tensor*, which estimates the curvatures per triangle instead of per vertex. The *curvature tensor,* which for a smooth surface is defined by the first-order partial derivatives of surface points and their normal vectors, is evaluated for each triangle by using linear interpolations between its vertices and their unit vector normal. As pointed out by Razdan and Bae in [26], this method satisfactorily evaluates the curvature only in the case of meshes with a uniform spacing between the vertices. Another face-based curvature estimator is proposed by Rusinkiewicz in [27]. This approach first computes the curvature tensor for each face and then estimates its value at each vertex (**p**) as a weighted average over the triangles incident to **p**.

For a smooth surface, the *curvature tensor* can be defined as:

$$\mathbf{\Pi} = (D_u \cdot \mathbf{n} \;\; D_v \cdot \mathbf{n}) = \begin{pmatrix} \frac{\partial \mathbf{n}}{\partial \mathbf{u}}\mathbf{u} & \frac{\partial \mathbf{n}}{\partial \mathbf{v}}\mathbf{u} \\ \frac{\partial \mathbf{n}}{\partial \mathbf{u}}\mathbf{v} & \frac{\partial \mathbf{n}}{\partial \mathbf{v}}\mathbf{v} \end{pmatrix} \tag{12}$$

where (**u**, **v**) are the directional of an orthonormal coordinate system in the tangent frame. Multiplying this tensor by any vector lying on the tangent plane, the derivative of the normal in that direction is obtained as:

$$\mathbf{\Pi} \cdot \mathbf{s} = D_s \cdot \mathbf{n} \tag{13}$$

In the case of triangular facets, Rusinkiewicz in [27] evaluates the *curvature tensor* by using finite differences:

$$\begin{cases} \mathbf{\Pi} \cdot \begin{pmatrix} \mathbf{e}_0 \cdot \mathbf{u} \\ \mathbf{e}_0 \cdot \mathbf{v} \end{pmatrix} = \begin{pmatrix} (\mathbf{n}_2 - \mathbf{n}_1) \cdot \mathbf{u} \\ (\mathbf{n}_2 - \mathbf{n}_1) \cdot \mathbf{v} \end{pmatrix} \\ \mathbf{\Pi} \cdot \begin{pmatrix} \mathbf{e}_1 \cdot \mathbf{u} \\ \mathbf{e}_1 \cdot \mathbf{v} \end{pmatrix} = \begin{pmatrix} (\mathbf{n}_0 - \mathbf{n}_2) \cdot \mathbf{u} \\ (\mathbf{n}_0 - \mathbf{n}_2) \cdot \mathbf{v} \end{pmatrix} \\ \mathbf{\Pi} \cdot \begin{pmatrix} \mathbf{e}_2 \cdot \mathbf{u} \\ \mathbf{e}_2 \cdot \mathbf{v} \end{pmatrix} = \begin{pmatrix} (\mathbf{n}_1 - \mathbf{n}_0) \cdot \mathbf{u} \\ (\mathbf{n}_1 - \mathbf{n}_0) \cdot \mathbf{v} \end{pmatrix} \end{cases} \tag{14}$$

where $\mathbf{e}_0$, $\mathbf{e}_1$ and $\mathbf{e}_2$ are the directions of the edges of the triangle and $\mathbf{n}_0$, $\mathbf{n}_1$ and $\mathbf{n}_2$ are the unit vectors normal at vertices (figure 4).

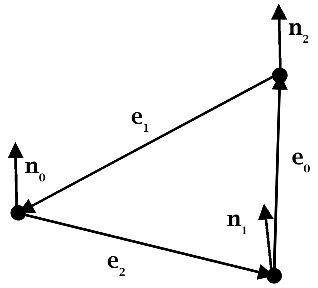


Fig. 4. Edges and normal directions used in the Rusinkiewicz's method [27] to build the *curvature tensor* of a triangle.

From the equation (14), for each triangle of the mesh $\mathbf{\Pi}$ is determined by using the least squares method. In order to evaluate the *curvature tensor* for each vertex **p**, a change of coordinate is carried out which transforms the *curvature tensor* of the triangles incident to **p** into the vertex coordinate frame, defined in the plane which is perpendicular to its normal. The weight used for averaging is the "Voronoi area" [21] associated with the triangle. The principal curvature and the corresponding principal directions at each vertex are evaluated as eigenvalue and eigenvectors of the tensor curvature.

The *Rusinkiewicz's* method indirectly takes into account the 2–ring neighborhood of **p**, by analyzing the variations to the unit vector normal at the vertices of each triangle incident to **p**.

## 4 VERTEX NORMAL ESTIMATION METHODS

Paraboloid fitting techniques and focal points' calculation need an accurate and robust estimation of the normal at vertex. In literature some criteria to estimate the normal at vertex are presented; some of them are hereunder described and analyzed. The methods here considered can be grouped into the following categories:

- the *weighted average*;
- the *tensor voting*;
- the *medial quadric;*
- the *Mean Curvature Normal.*

The first group of methods estimates the normal at vertex as the weighted average of the normal $\mathbf{n}_i$ of the triangles belonging to *1-ring neighborhood* of the vertex **p**:

$$\mathbf{n} = \frac{\sum_{i=1}^{nv} w_i \cdot \mathbf{n}_i}{\sum_{i=1}^{nv} w_i} \tag{15}$$

where $w_i$ are the weight factors. In literature various weighting criteria are proposed. Gouraud [9] introduced the *unweighted average* ($w_i$=1), which provides a vertex normal estimation which does not take into account the mesh's characteristics. Brown [3] considered the weights to be proportional to the areas of the triangles coming from **p** ($w_i$=$A_i$); however, this method does not take into account the shape of triangles (a thin and long triangle contributes as much as a wide and short one of equal area). Thürmer et al. [32] used weights which are proportional to the facet angles in **p** ($w_i$=$\theta_i$, see figure 1). Max [19] introduced the *sine angle-weighted average*, evaluated as follows (see Figure 1):

$$w_i = \frac{\sin\theta_i}{\|\mathbf{pp}_i\| \cdot \|\mathbf{pp}_{i+1}\|} \tag{16}$$

The *tensor voting* approach [20] evaluates, for each mesh vertex, the following matrix:

$$\mathbf{A} = \sum_{i=1}^{nv} w_i \cdot \mathbf{n}_i \cdot \mathbf{n}_i^{\,t} \tag{17}$$

where the weights $w_i$ are proportional to the areas of the triangles coming from **p** ($w_i$=$A_i$). In general **A** is symmetric and positive semi – definite and its eingenvalues are all real and nonnegative. ***A*** can be decomposed into

$$\mathbf{A} = \sum_{i=1}^{3} \lambda_i \cdot \mathbf{e}_i \cdot \mathbf{e}_i^{\,t} \tag{18}$$

where $\lambda_1 \geq \lambda_2 \geq \lambda_3$ are the eigenvalues of **A** and $\mathbf{e}_i$ are the corresponding eigenvector. According to this approach, $\mathbf{e}_1$ approximates the normal direction in **p**.

Jiao and Alexander [13] proposed the *medial quadric* approach for which, the normal estimation at each mesh vertex is obtained by minimizing the weighted sum of squared distances (*fundamental quadric*) of the triangles coming from **p** from **n**. This minimization is obtained by solving the following 3 x 3 linear system:

$$\mathbf{A} \cdot \mathbf{n} = -\mathbf{b} \tag{19}$$

where **A** is the same matrix reported in (14) and **b** is the following weighted average outward normal:

$$\mathbf{b} = \sum_{i=1}^{nv} w_i \cdot \mathbf{n}_i \tag{20}$$

The latter approach is based on the *Mean Curvature Normal* operator as shown in the formula (8).

As pointed out by Jiao and Alexander in [13], the best results can be obtained by the *medial quadric* method which is independent of the shape and dimension of the triangles of the 1 - ring neighborhood of the point analyzed. That is the reason why in the tests discussed in the following section the *medial quadric* criterion is used for vertex normal estimation.

## 5 EXPERIMENTAL RESULTS

In order to compare the methods for curvature estimation, some test cases are designed by using the following surface typologies: plane, cylinder, cone, sphere and torus. These are the most important typologies of surface to be recognized and, moreover, in this set of surfaces, all the point types (elliptic, flat, hyperbolic, parabolic and umbilical) can be found.

In Table I the geometrical differential parameters which are significant to recognize the type of point are reported. The quality of the mesh largely affects the performances of any curvature estimation method. In this work, in order to characterize some aspects concerning the quality of the mesh, the following parameters are introduced:

- $n_v(\boldsymbol{p})$ = *valence* of the 1 – *ring* neighborhood of **p**;
- $\mu(\boldsymbol{p}) H$ is a normalized measure of the mesh size in the neighborhood of **p,** where $\mu(\boldsymbol{p})$ is the mean size of the edges of the triangles belonging to the neighborhood;
- $\sigma(\boldsymbol{p})/\mu(\boldsymbol{p})$ is a normalized measure of the dispersion of the dimension of the triangles around **p**, where $\sigma(\boldsymbol{p})$ is the standard deviation of size of the edges of the triangles belonging to the neighborhood;
- $\theta_{max}$ = maximum angular value inside the 1-ring triangular facets around the target vertex **p**.

| **Point type** | **Relevant parameters** | **Monitored parameters** |
|---|---|---|
| *Flat (plane)* | *R* | *R* |
| *Parabolic (cylinder)* | *H, K,* $FS_{k1}$ | $\Delta_H$ *[%], K,* $\Delta_{FSk1}$ *[%]* |
| *Parabolic (cone)* | *H, K,* $FS_{k1}$ | $\Delta_H$ *[%], K,* $\Delta_{FSk1}$ *[%]* |
| *Umbilical (sphere)* | $\left\|H^2-K\right\|$, *H* | $\left\|H^2-K\right\|$, $\Delta_H$ *[%]* |
| *Elliptic - Hyperbolic (torus)* | $FS_{k1}$, $FS_{k2}$ | $\Delta_{FSk1}$ *[%],* $\Delta_{FSk2}$ *[%]* |

where:

$$\Delta_H[\%]=\left|\frac{H_{est}-H_t}{H_t}\right|*100$$;

$H_{est}$ is the estimated mean curvature;
$H_t$ is the nominal mean curvature;
$\Delta_{FSk1}$ = error of position of first focal point normalized on $k_1$;
$\Delta_{FSk2}$ = error of position of second focal point normalized on $k_2$

Tab. 1: The parameters monitored for each point type.

These parameters do not identify how well the triangular mesh approximates the original surface but they are, substantially, the parameters which affect the performance of the curvature estimation methods. A very significant and typical parameter that can be used to qualify a triangular mesh generated from a regular surface is the SAG, that is to say, the maximum value of the distance from the barycenter of a mesh triangle to the original surface. As evidenced by the experimental tests conducted in this work, the performances of the curvature estimation methods are not affected by this parameter. If we are to generalize from the results obtained, parameters and evaluated errors must be normalized so that they can be extended to similar cases.

Experimental tests are conducted for different synthetic meshes characterized by selected values of the mesh quality parameters and for synthetic meshes with random error added ($\delta_{err}$). The experimental tests carried out in this work have been designed by following a standard approach, which consists of varying one parameter at a time, keeping all other parameters at the base-case value ($n_v(\mathbf{p})$ = 6; $\mu(\mathbf{p})$ = 1 mm; $\sigma(\mathbf{p})$ = 0 mm; $\theta_{max}$ =60°, $\delta_{err}$ = 0 mm). In Table II, the levels' number and the increment step, or straightforwardly the corresponding values of the analyzed parameters, are quoted for each type of point being analyzed. The curvature estimation methods which have been analyzed are the *Meyer discrete method*, the *simple quadric*, the *extended quadric* and the *Rusinkiewicz fitting methods*. The performance of the last-named is evaluated by using *Rusinkiewicz's* implementation (http://www.cs.princeton.edu/gfx/proj/trimesh2/) and by analyzing 2-ring neighborhoods. After a preliminary experimentation, the *full quadric fitting method* has been discarded due to its instability for low values of the *valence* and to the large errors evidenced. In the next sub-sections a summary of some of the most significant results are described. Each of the next sub-sections refers to a specific factor which identifies the quality of the mesh.

| **Parameters** \ **Point types** | | Flat *(plane)* | Parabolic (uniform curvatures) *(cylinder)* | Parabolic (non uniform curvatures) *(cone)* | Umbilical *(sphere)* | Elliptic and Hyperbolic *(torus)* |
|---|---|---|---|---|---|---|
| $\mu(\mathbf{p})$ $H(^*)$ | *n° of levels* | 26 | 26 | 26 | 26 | 14 |
| | *initial value* | 0.25 mm | 0.0039 | 0.0039 | 0.012 | 0.015 |
| | *step* | 0.25 mm | 0.0039 | 0.0039 | 0.012 | 0.015 |
| $\sigma(\mathbf{p})/\mu(\mathbf{p})$ | *n° of levels* | 8 | 8 | 8 | 7 | 15 |
| | *values* | 0, 0.002, 0.086, 0.171, 0.184, 0.248, 0.314, 0.420 | 0, 0.0001, 0.0055, 0.0106, 0.0115, 0.0156, 0.0193, 0.0261 | 0, 0.007, 0.011, 0.012, 0.015, 0.017, 0.019, 0.021 | 0, 0.0043, 0.0085, 0.0128, 0.0170, 0.0212, 0.0253 | 0, 0.0454, 0.1196, 0.158, 0.1963, 0.2346, 0.2727, 0.3105, 0.3481, 0.3854, 0.4224, 0.4592, 0.4957, 0.532, 0.5681 |
| $n_v(\mathbf{p})$ | *n° of levels* | 9 | | | | |
| | *values* | 5, 6, 8, 10, 12, 14, 16, 18, 20 | | | | |
| $\theta_{max}$ [°] | *n° of levels* | 7 | | | | |
| | *values* | 60, 70, 80, 90, 100, 120, 140 | | | | |
| $\delta_{err}$ | *n° of levels* | 7 | | | | |
| | *values* | 0.003, 0.005, 0.01, 0.025, 0.03, 0.04, 0.05 | | | | |

(*) $\mu(\mathbf{p})$ for flat point;
the i-th level of parameter value is obtained as: initial_value + (i-1)*step, for i=1,2,…..,n° of levels.

Tab. 2: Experimental tests: levels' number and parameters' values for each type of point analyzed.

### 5.1 Valence of the 1-ring Neighborhood of p

A set of experiments have been conducted selecting neighborhoods of **p** having different values for the *valence*: from 3 to 20. As far as the *fitting* methods are concerned, in all the cases analyzed the *extended quadric* does not seem to be significantly affected by the *valence* (figure 5), whereas the *simple quadric* is unstable for $n_v$ =3 and the *Rusinkiewicz*'s method proves to be quite sensitive to this factor. By contrast, *Gauss-Bonnet* based discrete methods are largely sensitive to the *valence*, as noticed also by Gatzke and Grimm [7]. Borrelli et al. [2] proved that, at what they call *regular vertex,* these methods have their minimum sensitive for $n_v$ equal to 6. They also pointed out that, for $n_v \neq 6$, angular defect is not just a function of Gaussian curvature but also of principal curvature values. All these considerations have been confirmed by the results of the experiments, as it is shown in figure 5, which refers to the error in the focal points' evaluation in a torus.

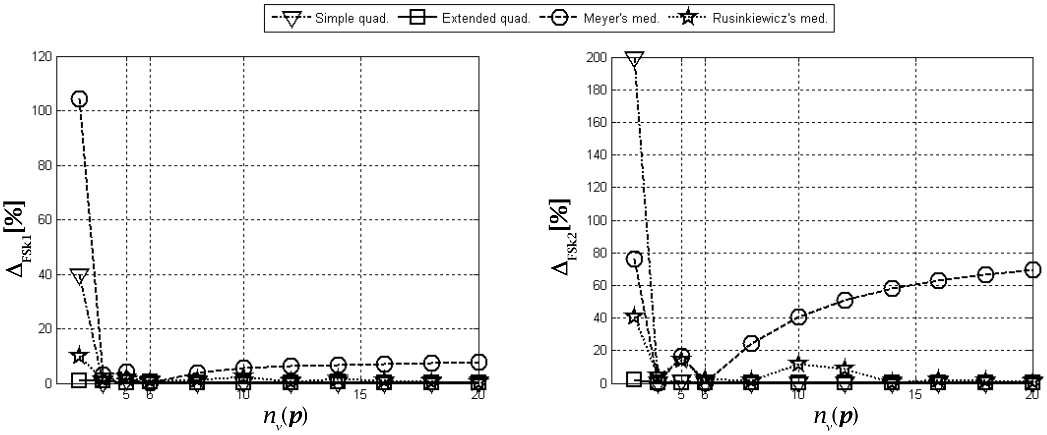


Fig. 5: Impact of the valence on the error in the focal point estimation for a tessellated torus.

### 5.2 Maximum angular value $\theta_{max}$

The maximum angular value inside the triangular facets around the vertex **p** affects the error in curvature estimation. This factor has greater relevance in *Gauss-Bonnet* based discrete methods than in fitting ones. In particular, for angle values greater than *90°*, *Meyer method* produces very large errors in curvature estimation. On the contrary, paraboloid *fitting methods* do not seem to be sensitive to this factor. Figure 6 shows the impact of the $\theta_{max}$ on the parameter $H^2$-$K$, suited for sphere recognition. Analogous results have been obtained for other kinds of geometries. Meyer's attempt at solving the problem derived from obtuse angles by introducing a properly chosen integration region does not yield useful results: the error in *H* and *K* estimation, for $\theta_{max}>90°$, can reach such high values (see Figure 6) that it practically makes *Meyer method* unusable. The *Rusinkiewicz*'s method proves to be sensitive to this factor in the case of a strong distortion of the 2–ring neighborhood ($\theta_{max}>120°$).

### 5.3 Mesh dimension in the 1-ring neighborhood

Mesh dimension is another important factor which affects the error of curvature estimation methods. Two different contributions to the error can be identified: the first one due to the mean values of the dimension of triangles incident to **p** and the second one owing to the dispersion in the triangles' dimensions. Both these contributions have been analyzed by means of two different sets of numerical experiments.

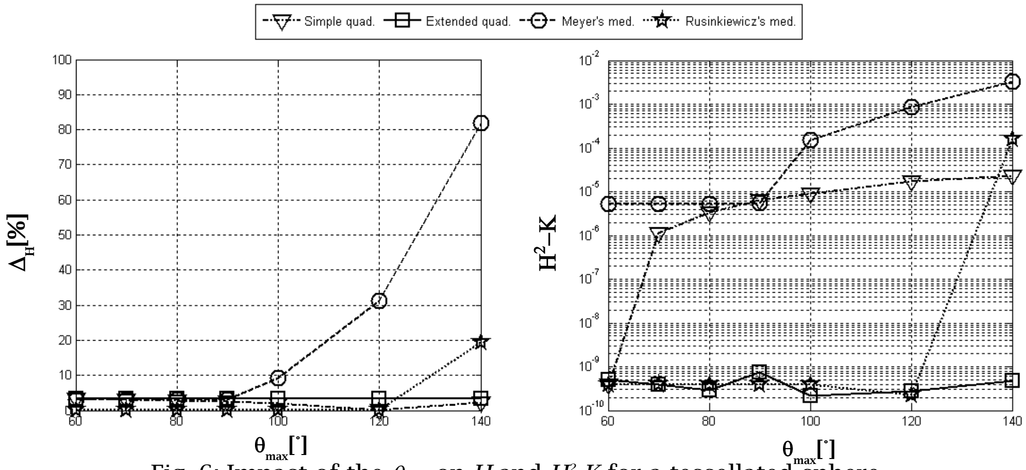


Fig. 6: Impact of the $\theta_{max}$ on $H$ and $H^2$-$K$ for a tessellated sphere.

The first contribution of the mesh dimension has been analyzed by processing regular meshes which do not have dispersion in the values of the triangles' dimensions. For $n_v$ = 6 and for all the geometries analyzed, *simple* and *extended quadric methods* show greater sensitivity to mesh dimensions than the *Meyer* and *Rusinkiewicz methods* (see Figure 7). This is due to the properties of the fitting surface used to evaluate curvatures. Paraboloid performs a polynomial approximation of points in $N_1(\mathbf{p})$; the computed curvatures are not so accurate when the points lie on a surface that is represented by a rational function (as in the case of an axial symmetric surface). It is important to notice that, for the recognition of the type of point, the relative values of the principal curvatures are more important than their absolute values; therefore, there are not significant problems in point recognition when the paraboloid *fitting method* is used. By contrast, in focal point evaluation, the absolute values of the curvature are essential to obtain useful results.

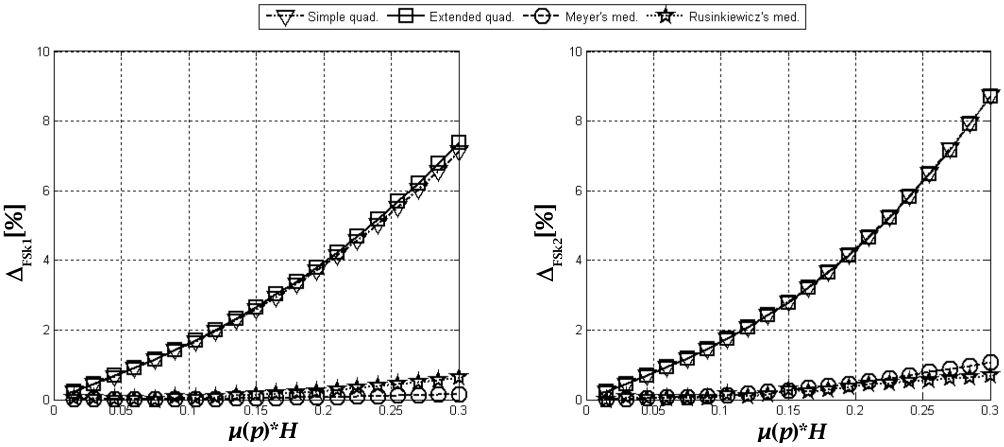


Fig. 7: Impact of $\mu(\boldsymbol{p})\cdot H$ on the error in estimated focal points' location for a tessellated torus.

The second contribution of the mesh dimension has been analyzed by processing meshes characterized by dispersion in the dimensions of triangles incident to **p**, leaving out the cases with obtuse angles, which have been separately analyzed since they affect the performance of the *Meyer method*. The *simple quadric fitting method* seems to be very sensitive to dispersion in the dimensions of triangles with an unstable behavior (see Figures 8 and 10). In comparison, the *extended quadric* appears to be stable and not significantly affected by this factor. The *Meyer method* proves to be quite sensitive to dispersion in the dimensions of triangles. The *Rusinkiewicz's* method, in turn, does not seem to be significantly affected by this factor but, unlike the other methods, the error in curvature estimation is noticeably affected by the orientation of the mesh with respect to principal directions. The configurations I and II shown in figure 8 refer to those depicted in figure 9.

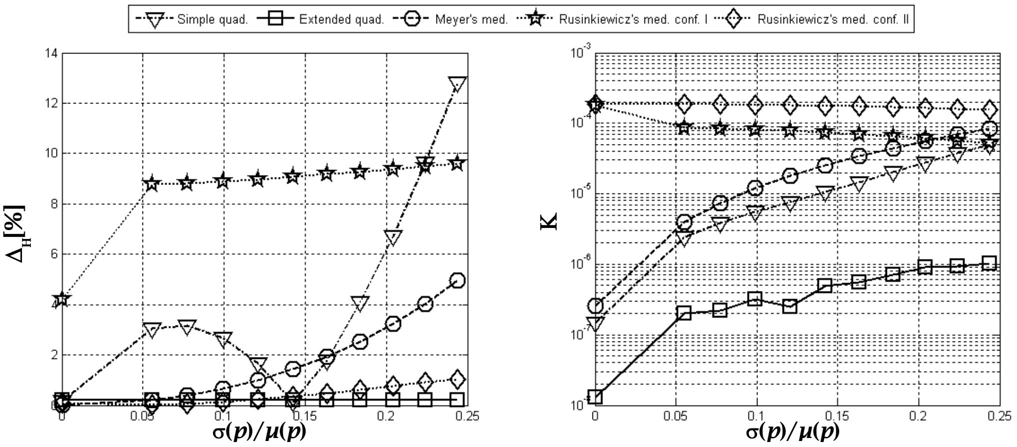


Fig. 8: Impact of $\sigma(\boldsymbol{p})/\mu(\boldsymbol{p})$ on H and K estimation (tessellated cone: $\mu(\boldsymbol{p}) \cdot H = 0.0485$, $n_v(\boldsymbol{p}) = 6$).

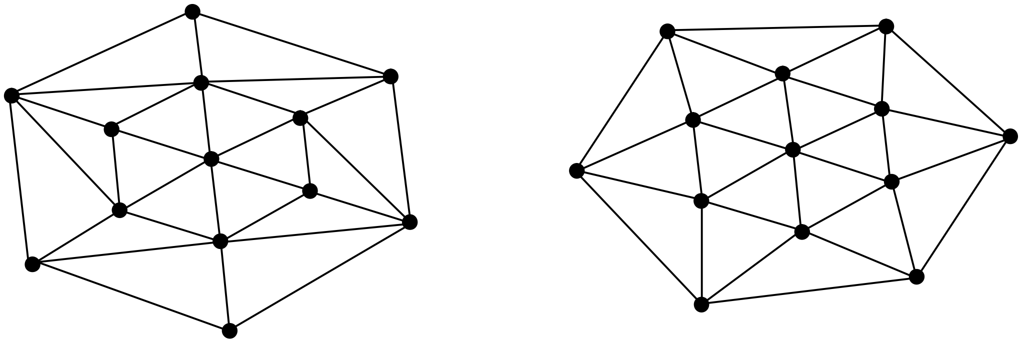

**Configuration I** **Configuration II**

Fig. 9: Two different configurations of the 2-ring neighborhood used when analyzing the performance of the *Rusinkiewicz's* method.

## 5.4 Noise in point location

The noise affecting point location can be detected in all the meshes obtained by a scanning process of a real object. This noise strictly affects any curvature estimation process. The test cases here used to analyze curvature estimation methods have been generated from synthetic meshes with random error added. The random error is applied by producing a displacement of the vertex, normal to the surface. The value of the displacement for each vertex is randomly generated with a normal probability density function. The results of the experimental tests related to meshes affected by errors have been evaluated as the mean values of groups of 30 experiments analyzed for each test case. In figures 11 and 12 the results are represented; $\delta_{err}$ is the measure of the noise evaluated as the maximum distance of the points in $N_1(\mathbf{p})$ in the direction of the normal vector $\mathbf{n}(\mathbf{p})$. For the *simple* and the *extended quadric* and for the *Meyer* method, the estimated value for the *R* parameter (which is the parameter suited to the recognition of planar faces) is over *0.008* for a noise level of $\delta_{err}/\mu(\boldsymbol{p})=0.03$ (see Figure 11).

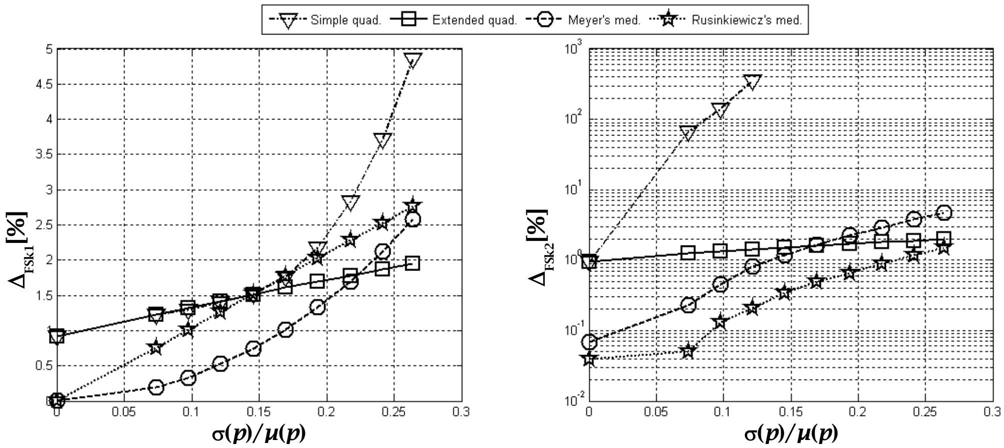


Fig. 10. Impact of □(***p***)/*μ*(***p***) on the error in the estimated focal points' location (tessellated torus: *μ*(***p***)□*H = 0.06, $n_v$*(***p***)=*6*).

This value of *R* is also compatible with non-planar surfaces, for a noise level (*$\delta_{err}/\mu$*(***p***)*=0.03*) that is lower than the typical level detected in scanned surfaces that are not pre-smoothed. For these same methods (that is, *simple* and *extended quadric* and *Meyer's*) and a level of noise (*$\delta_{err}/\mu$*(***p***)*=0.03* ) the estimated value of *K* in a cylindrical surface (diameter *64mm*) is *$1.393{*}10^{-3}$*, which is also compatible with a sphere having a diameter of *26.8 mm*. It is important to notice that the value of the parameter *$H^2$-K*, used to recognize umbilical points is, in this specific case, *$1.18{*}10^{-6}$* and that practically it is not very far from the values measured in synthetic meshes of a sphere (see Figure 6). For these reasons, all the methods which use the first ring neighborhood have so high a sensitivity to noise that practically cannot be used to estimate curvatures or to recognize the type of point. The *Rusinkiewicz's* method turns out to be the least sensitive to noise level, but it is important to highlight the fact that it takes into account the 2–ring neighborhood of the point, performing an intrinsic smoothing of the surface data. For the previously defined noise levels and point types, the values of R and K are 0.003027 and *$4.341{*}10^{-4}$* respectively. The value of K could not make possible the correct recognition of a cylindrical face.

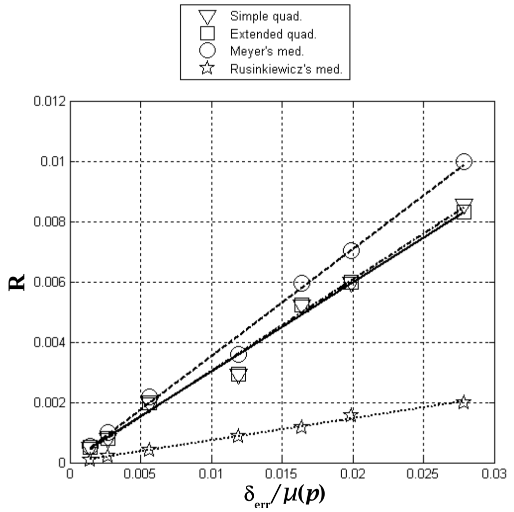


Fig. 11. Impact of $\delta_{err}/\mu$(***p***) on *R* for tessellated planes.

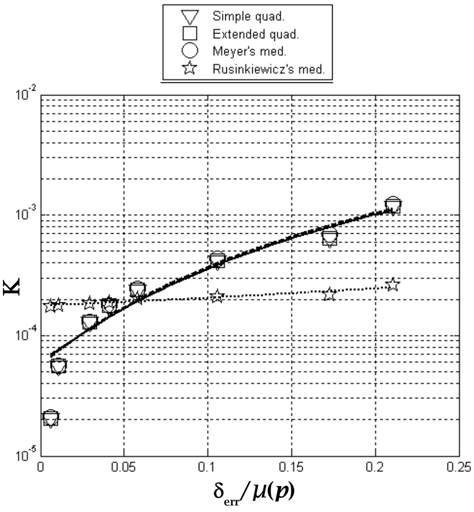


Fig. 12. Impact of $\delta_{err}/\mu$(***p***) on *K* for tessellated cylinders.

The paraboloid *fitting methods* can be applied using higher orders of ring neighborhood. In Tables III and IV the values of $R$ and $K$ are reported for different orders of ring neighborhood: from 1 to 3. The values of $R$ and $K$ rapidly fall to values that clearly and respectively distinguish, in the practical situation, a plane or a ruled surface from any other kind of geometry. When comparing the *extended quadric* with the *Rusinkiewicz's* method, both of which evaluate the same neighborhood order, it is manifest that the former proves to yield better results.

| | $(\delta_{err}/\mu(\boldsymbol{p}) = 0.03)$ | | |
|---|---|---|---|
| | $N_1(\boldsymbol{p})$ | $N_2(\boldsymbol{p})$ | $N_3(\boldsymbol{p})$ |
| $R$ | 0.008163 | 0.002542 | 0.000698 |

Table III. The impact of the ring – neighborhood order of the point p on the R evaluation of a noised planar mesh

| | $(\delta_{err}/\mu(\boldsymbol{p}) = 0.03)$ | | |
|---|---|---|---|
| | $N_1(\boldsymbol{p})$ | $N_2(\boldsymbol{p})$ | $N_3(\boldsymbol{p})$ |
| $K$ | $1.393*10^{-4}$ | $2.249*10^{-5}$ | $2.088*10^{-6}$ |

Table IV. The impact of ring – neighborhood order of the point p on the *K* evaluation of a noised cylindrical mesh

## 6 CONCLUSIONS

In this work an investigation about the stability and accuracy of the most important shape recognition methods for tessellated objects is carried out. In order to highlight the effects of mesh parameters such as resolution, regularity and noise, four methods (two paraboloid fitting ones, Rusinkiewicz's and Meyer's) have been investigated by means of a set of specifically designed test cases.

On the one hand, paraboloid *fitting methods* prove to be affected mainly by the mesh dimension. Error in curvature estimation can be detected, which increases as the mesh dimension increases. This error does not significantly compromise the identification of point type when it involves recognizing null values in some characteristic parameters. It is the case of $R$, $H^2$-$K$ and $K$ parameters. On the other hand, paraboloid *fitting methods* produce errors, which are larger as the mesh dimension increases, when evaluating quantitative parameters such as focal points and mean curvature. The *simple quadric method* is unstable for valence = 3 (see Figures 5) and highly sensitive to mesh dispersion of the dimensions of *1-ring neighborhood* (see Figures 8 and 10). It is for this reason that the *simple quadric method* cannot be used in a practical situation when dispersion in the triangles' dimension is very frequent.

Regarding synthetic meshes, *Rusinkiewicz's method* falls short since it is affected by the orientation of the mesh with respect to principal directions. Furthermore, these methods have difficulty in evaluating the differential geometric parameters in vertices near non–regular points.

The *Meyer method* shows some critical states that are typical of all *Gauss-Bonnet* based *discrete methods*. These critical states manifest for *valence* not equal to six and for a high dispersion in the mesh dimension in the *1-ring neighborhood*. A specific critical state of the *Meyer method* manifests when there are obtuse triangles. In this case, the method produces large error in the estimation of any geometrical differential parameter. It is important to notice that *valence* different from six and obtuse triangles can be commonly found in real cases of meshes generated by reverse engineering and also in synthetic meshes. It is, for example, the case of the benchmark proposed by Hugues Hoppe, which is shown in figure 13. In the geometric model of an oil pump housing, the points having *valence* different from six (see Figure 13 b) and obtuse triangles (see Figure 13 c) are illustrated. As it can be observed in the case in figure 12, and also in many other practical cases, obtuse triangles and *valence* different from six are located in many parts of the geometric model. In the geometric model in figure 13 the percentage of the area of the obtuse triangles is *48.4%.* The large error the *Meyer method* produces in these zones gives rise to such high uncertainty in point type recognition that it cannot be used for this purpose. The test cases used in literature to analyze *Meyer method* are not focused on shape recognition and do not refer to real practical cases affected by error in points' location.

The results of many of the test cases analyzed show that those methods which use the *1 - ring neighborhood* have high sensitivity to noise, and hence, cannot be practically used to estimate curvatures or to recognize the type of point in scanned surfaces. The *Rusinkiewicz's method* shows a satisfactory performance depending on the type of point and only for certain neighborhood vertex arrangements. The *extended quadric fitting method* shows quite a good capability, independently from the point type, when the neighborhood order is higher than the first one. On the other side some problems occur when evaluating quantitative parameters such as the absolute location of focal points or curvature measures. As far as point type recognition is concerned (elliptic, flat, hyperbolic, parabolic and umbilical), the relative values of the principal curvatures are more important than their absolute values and for this goal *extended quadric fitting method* performs good results.

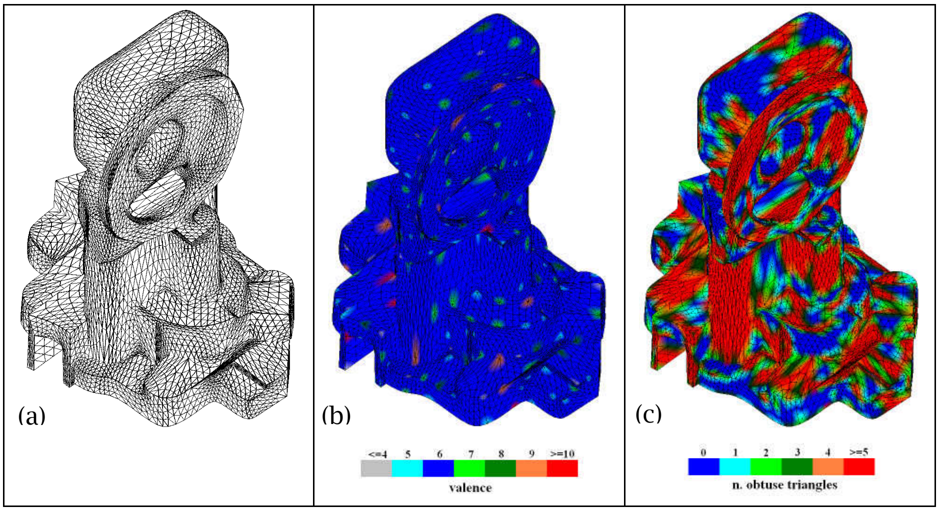


Fig. 13. Quality of the mesh (valence (b) and obtuse triangles (c)) of a typical mesh of a scanned object (a).

**REFERENCES**

[1] Agam, G., and Tang, X.: A Sampling Framework For Accurate Curvature Estimation In Discrete Surfaces, IEEE Transactions On Visualization And Computer Graphics, 11 (5), 2005, 573-583.
[2] Borrelli, V., Cazals, F., Morvan, J.M: On The Angular Defect Of Triangulations And The Pointwise Approximation Of Curvatures, Computer Aided Geometric Design, 20 (6), 2003, 319-341.
[3] Brown, J.L.: Vertex Based Data Dependent Triangulations, Computer-Aided Design, 8 (3), 1991, 239-251.
[4] Chen, X. And Schmitt, F.: Intrinsic Surface Properties From Surface Triangulation, In Proceedings Of European Conference On Computer Vision, 1992, 739-743.
[5] Cohen-Steiner, D. and Morvan, J.: Restricted Delaunay Triangulations And Normal Cycle, In Proceedings Of 19th Annual Acm Symposium On Computational Geometry, 2003, 237-246.
[6] Do Carmo, M. P.: Differential Geometry Of Curves And Surfaces, Prentice-Hall, Englewood Cliffs, 1974, N J.
[7] Gatzke T., And Grimm, C.: Estimating Curvature On Triangular Meshes, International Journal Of Shape Modeling, 12 (1), 2006, 1-29. doi:10.1142/S0218654306000810
[8] Goldfeather, J. and Interrante, V.: A Novel Cubic-Order Algorithm For Approximating Principal Direction Vectors. Acm Transactions On Graphics, 23 (1), 2004, 45-63.

[9] Gouraud, H.: Continuous Shading Of Curved Surfaces. Ieee Transaction On Computers, 20 (6), 1971, 623-629. doi:10.1109/T-C.1971.223313

[10] Hamann, B.: Curvature Approximation For Triangulated Surfaces, In Geometric Modelling, G. Farin, H. Hagen, H. Noltemeier And W. Knödel, Springer Verlag, 1993, 139–153.

[11] Hameiri, E. and Shimshoni I.: Estimating The Principal Curvatures And The Darboux Frame From Real 3d Range Data. In Proceedings Of 3d Data Processing Visualization And Transmission Symposium, 2002, 258-267.

[12] Hoppe, H., Microsoft Research, (www.Cs.Caltech.Edu/~Njlitke/Meshes/ Collections/ Hhoppe/)

[13] Jiao, X., Alexander, P. J.: Parallel Feature-Preserving Mesh Smoothing. In International Conference On Computational Science And Its Applications (4), 2005, 1180–1189.

[14] Krsek, P., Lukics, C., Martin, R. R.: Algorithms For Computing Curvatures From Range Data. In The Mathematics Of Surfaces Viii , R. Cripps Ed., Information Geometers, 1998, 1-6.

[15] Lin, C., And Perry, M.: Shape Description Using Surface Triangulation, In Proceedings Of IEEE Workshop On Computer Vision, Representation And Control, Rindge, Nh., 1982, 38÷43.

[16] Lipshitz, B. And Fischer A., Verification Of Scanned Engineering Parts With Cad Models Based On Discrete Curvature Estimation. In Proceedings Of Shape Modeling Applications, 2004, 333-336.

[17] Magid, E., Soldea, O., Rivlin, E.:A Comparison of Gaussian and mean curvature estimation methods on triangular meshes of range image data. Computer Vision and Image Understanding, 107 (3), 2007, 139-159. doi:10.1016/j.cviu.2006.09.007

[18] Martin, R.R.: Estimation Of Principal Curvatures From Range Data. International Journal Shape Modeling, 4 (3/4), 1998, 99-109. doi:10.1142/S0218654398000088

[19] Max, N.: Weights For Computing Vertex Normals From Facet Normals. Journal Of Graphics Tools, 4 (2), 1999, 1-6.

[20] Medioni, G., Lee, M. S., Tang, C. K.: A Computational Frame Work For Segmentation And Grouping. Elsevier, 2000, Amsterdam.

[21] Meyer, M., Desbrun, M., Schroeder, P., And Barr, A.: Discrete Differential Geometry Operators For Triangulated 2-Manifolds. In Visualization And Mathematics Iii, H. C. Hege And K. Polthier, Eds. Springer-Verlag, Heidelberg, 2003, 35÷57.

[22] Mizoguchi, T., Date, H., Kanai, S. And Kishinami, T.: Segmentation Of Scanned Mesh Into Analytic Surfaces Based On Robust Curvature Estimation And Region Growing. In Proceedings Of Geometric Modelling And Processing, 2006, 644-654.

[23] Mortenson, M. E.: Geometric Modeling, John Wiley & Sons, 1982, New York.

[24] Page, D. L., Koschan, A., Sun, Y., Paik, J. And Abidi, A.: Normal Vector Voting: Crease Detection And Curvature Estimation On Large, Noisy Meshes. Graphical Models, 64(3/4), 2002, 199–229.

[25] Petitjean, S.: A Survey Of Methods For Recovering Quadrics In Triangle Meshes. Acm Computing Surveys, 2 (34), 2002, 1-61.

[26] Razdan, A., And Bae, M.: Curvature Estimation Scheme For Triangle Meshes Using Biquadratic Bézier Patches. Computer-Aided Design, 37 (14), 2005, 1481-1491.

[27] Rusinkiewicz, S.: Estimating Curvatures And Their Derivatives On Triangle Meshes, In Proceedings Of 2nd International Symposium On 3d Data Processing, Visualization And Transmission, September 06-09 2004, 486-493.

[28] Song, H., Feng, H. Y., Ouyang, D: Automatic Detection Of Tangential Discontinuities In Point Cloud Data. Journal Of Computing And Information Science In Engineering, 8 (2), 2008.

[29] Surazhsky, T., Magid, E., Soldea, O., Elber, G. And Rivlin E.: A Comparison Of Gaussian And Mean Curvatures Estimation Methods On Triangular Meshes. In Proceedings Of 2003 IEEE International Conference On Robotics & Automation, Taipei, Taiwan, September 14÷19, 2003.

[30] Taubin, G.: Estimating The Tensor Of Curvature Of A Surface From A Polyhedral Approximation, In Proceedings Of International Conference Of Computer Vision, 1995, 902-907.

[31] Theisel, H., Rossl, C., Zayer, R., And Seidel, H. P.: Normal Based Estimation Of The Curvature Tensor For Triangular Meshes, In Proceedings Of 12th Pacific Conference On Computer Graphics And Applications, 2004, 288-297.

[32] Thürmer, G., And Wüthrich, C.: Computing Vertex Normals From Polygonal Facets. Journal Of Graphics Tools, 3 (1), 1998., 43-46.

[33] Tong, W. S., And Tang, C. K.: Robust Estimation Of Adaptive Tensors Of Curvature By Tensor Voting. IEEE Transactions On Pattern Analysis And Machine Intelligence, 27 (3), 2005, 434-449.

[34] Xu, G.: Convergence Analysis Of A Discretization Scheme For Gaussian Curvature Over Triangular Surfaces. Computer-Aided Design, 23 (2), 2006, 193-207.